Article

Radical Cage Effects in the Photochemical Degradation of Polymers: Effect of Radical Size and Mass on the Cage Recombination Efficiency of Radical Cage Pairs Generated Photochemically from the (CpCHCHN(CH)C(O)(CH)CH)Mo(CO) (*n* = 3, 8, 18) Complexes

Erick Schutte, T. J. R. Weakley, and David R. Tyler

J. Am. Chem. Soc., **2003**, 125 (34), 10319-10326• DOI: 10.1021/ja035030r • Publication Date (Web): 31 July 2003

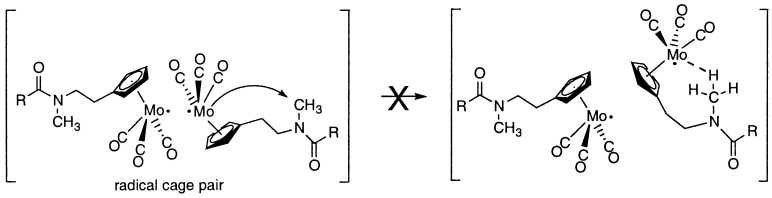

More About This Article

Additional resources and features associated with this article are available within the HTML version:

- Supporting Information
- Links to the 2 articles that cite this article, as of the time of this article download
- Access to high resolution figures
- Links to articles and content related to this article
- Copyright permission to reproduce figures and/or text from this article

View the Full Text HTML

J|A|C|S
ARTICLES
Published on Web 07/31/2003

Radical Cage Effects in the Photochemical Degradation of Polymers: Effect of Radical Size and Mass on the Cage Recombination Efficiency of Radical Cage Pairs Generated Photochemically from the $(CpCH_2CH_2N(CH_3)C(O)(CH_2)_nCH_3)_2Mo_2(CO)_6$ (n = 3, 8, 18) Complexes

Erick Schutte, T. J. R. Weakley, and David R. Tyler*

Contribution from the Department of Chemistry, University of Oregon, Eugene, Oregon 97403

Received March 6, 2003; E-mail: dtyler@darkwing.uoregon.edu

Abstract: This study explored the effect of radical size, chain length, and mass on the cage recombination efficiency of photochemically generated radical cage pairs. Radical cage pairs containing long-chain radicals of the type [$(CpCH_2CH_2N(CH_3)C(O)(CH_2)_nCH_3)(CO)_3Mo\bullet$, $\bullet Mo(CO)_3(CpCH_2CH_2(CH_3)NC(O)(CH_2)_nCH_3)$] were generated in hexanes/squalane solution by photolysis (λ = 546 nm) of the Mo−Mo bonds in $(CpCH_2CH_2N(CH_3)C(O)(CH_2)_nCH_3)_2Mo_2(CO)_6$ (n = 3, 8, 18). The cage recombination efficiencies (denoted as F_{cP}, where $F_{cP} = k_{cP}/(k_{cP} + k_{dP})$, k_{dP} is the diffusion rate constant, and k_{cP} is the radical recombination rate constant) for the radical cage pairs were obtained by extracting them from quantum yield measurements for the photoreactions with CCl_4 (a metal-radical trap) as a function of solvent system viscosity. The results show that F_{cP} increases as the length of the chain on a radical center increases. This finding likely provides at least one of the reasons why the quantum yields for photolytic polymer degradation (and long-chain molecules, in general) decrease as the polymer chains get longer. In quantitative terms, plots of k_{dP}/k_{cP} were linearly proportional to mass$^{1/2}$/radius^2, in agreement with the prediction of Noyes' cage effect theory. The "radius" of a long-chain radical, such as those studied herein, is rather vague, and for that reason a less ambiguous structural parameter was sought to replace the r^2 term in the Noyes expression. Plots of k_{dP}/k_{cP} vs mass$^{1/2}$/surface area suggest that surface area can be used in place of the radius^2 term in the Noyes expression. The significance of being able to use a particle's surface area in the Noyes expression is that the expression becomes useful for nonspherical particles. The new expression allows the approximate prediction of F_{cP} values for radicals of different sizes and masses.

Introduction

Photochemically reactive polymers[1−3] are of considerable interest because they are useful as degradable plastics,[4] photoresists,[5−9] biomedical materials, and as precursors to ceramic materials.[5−7,10−13] To expand the repertoire of photodegradable polymers, we have been developing a new class of polymers that contain metal−metal-bonded organometallic dimers interspersed along the polymer backbone.[14−16] These polymers are photodegradable because the metal−metal bonds can be cleaved with visible light and the resulting metal radicals captured with oxygen or other traps (Scheme 1).[17]

In a recent paper, we showed that the overall quantum yields for the degradation of these polymers and their model complexes varied as a function of molecular weight and size.[15] Reasons for the dependence of the quantum yields on the chain length have been a matter of considerable interest and speculation.[18,19]

(1) (a) Grassie, N.; Scott, G. *Polymer Degradation and Stabilization*; Cambridge University Press: New York, 1985. (b) Guillet, J. *Polymer Photophysics and Photochemistry*; Cambridge University Press: Cambridge, U.K., 1985.
(2) Rabek, J. F. *Mechanisms of Photophysical Processes and Photochemical Reactions in Polymers*; Wiley: New York, 1987.
(3) Geuskens, G. *Comprehensive Chemical Kinetics*; Bamford, C. H., Tipper, C. F. H., Eds.; Elsevier: New York, 1975; Vol. 14, pp 333−424.
(4) Guillet, J. E. *Degradable Materials*; Barenberg, S. A., Brash, J. G., Narayan, R., Redpath, A. E., Eds.; CRC Press: Boston, MA, 1990; pp 55−97.
(5) West, R.; Maxka, J. *Inorganic and Organometallic Polymers*; Zeldin, M., Wynne, K. J., Allcock, H. R., Eds.; ACS Symposium Series 360; American Chemical Society: Washington, DC, 1988; Chapter 2.
(6) West, R. *Actual. Chim.* **1984**, 64.
(7) West, R. *J. Organomet. Chem.* **1986**, *300*, 327.
(8) Hoger, D. C.; Miller, R. D.; Wilson, C G.; Neureuther, A. R. *Proc. SPIE-Int. Soc. Opt. Eng.* **1984**, *469*, 108.
(9) Ishikawa, M.; Nate, K. *Inorganic and Organometallic Polymers*; Zeldin, M., Wynne, K. J., Allcock, H. R., Eds.; ACS Symposium Series 360; American Chemical Society: Washington, DC, 1988; Chapter 16.
(10) Yajima, S.; Hayashi, J.; Omori, M. *Chem. Lett.* **1975**, 931.
(11) Yajima, S. *Ceram. Bull.* **1983**, *62*, 893.
(12) Laine, R. M.; Blum, Y. D.; Tse, D.; Glaser, R. *Inorganic and Organometallic Polymers*; Zeldin, M., Wynne, K. J., Allcock, H. R., Eds.; ACS Symposium Series 360; American Chemical Society: Washington, DC, 1988; Chapter 10.
(13) Gilead, D. *Degradable Materials*; Barenberg, S. A., Brash, J. G., Narayan, R., Redpath, A. E., Eds.; CRC Press: Boston, MA, 1990; pp 191−207.
(14) (a) Tenhaeff, S. C.; Tyler, D. R. *Organometallics* **1991**, *10*, 473−482. (b) Tenhaeff, S. C.; Tyler, D. R. *Organometallics* **1991**, *10*, 1116−1123.
(15) Tenhaeff, S. C.; Tyler, D. R. *Organometallics* **1992**, *11*, 1466−1473.
(16) Niekarz, G. F.; Tyler, D. R. *Inorg. Chim. Acta* **1996**, *242*, 303−310.
(17) (a) Meyer, T. J.; Caspar, J. V. *Chem. Rev.* **1985**, *85*, 187. (b) Geoffroy, G. L.; Wrighton, M. S. *Organometallic Photochemistry*; Academic Press: New York, 1979.

Scheme 1. Photochemical Degradation of a Polymer with Metal−Metal Bonds along Its Backbone

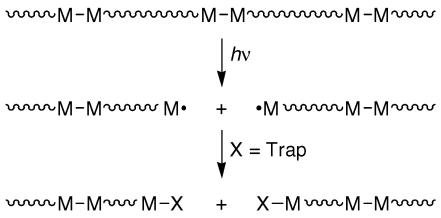

Scheme 2. Reaction Scheme for Metal−Metal Bond Photolysis

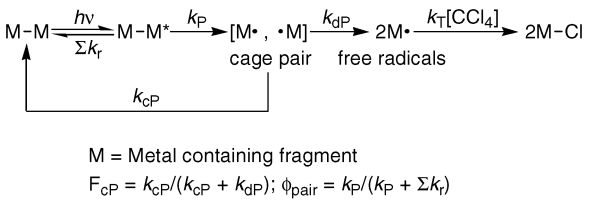

M = Metal containing fragment

$F_{cP} = k_{cP}/(k_{cP} + k_{dP})$; $\phi_{pair} = k_P/(k_P + \Sigma k_r)$

One hypothesis speculates that the dependence is attributable to the radical cage effect, specifically to changes in the "cage recombination efficiency" as the chain length is varied (Scheme 2).[20] The "cage recombination efficiency" (denoted as F_c and colloquially known as the "cage effect") is defined as the ratio of the rate constant for cage recombination to the sum of the rate constants for all competing cage processes. (The F_c value for a photochemically formed cage pair does not necessarily equal F_c for the same cage pair formed by thermolysis or by diffusional collision of two free radicals.[21] To differentiate these cases, the photochemical cage efficiency will be denoted F_{cP} and the associated rate constants as k_{cP} and k_{dP}. In the photolysis reaction in Scheme 2, $F_{cP} = k_{cP}/(k_{cP} + k_{dP})$.)

To gain greater insight into the role that F_{cP} plays in controlling the degradation of polymers, we synthesized and studied the series of model complexes $(CpCH_2CH_2OSiR_3)_2Mo_2(CO)_6$ (R = Me, *i*-Pr, *n*-Pr, *n*-Hx) and determined that the cage effect was indeed dependent on the size and mass of the radical fragments.[22] Specifically, k_d/k_c was linearly proportional to $m^{1/2}/r^2$ (where m is the mass of the radical and r its radius). This result represented the first experimental verification of Noyes's prediction concerning the relationship of particle mass and size to the cage effect.[23]

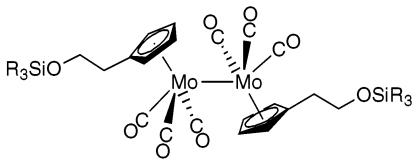

R = Me, *n*-Pr, *i*-Pr, *n*-Hx

To study the generality of this result, we next synthesized and studied the cage effects in the model complexes $(CH_3(CH_2)_nC(O)NHCH_2CH_2Cp)_2Mo_2(CO)_6$ (n = 3, 8, 13, 18) (**1**−**1** to **4**−**4**).[24] (The numbers assigned to these dimers are used to facilitate discussion of their cage pairs. Thus, the radical cage pair for dimer **1**−**1** becomes [**1**•, •**1**], etc.)

Scheme 3. In-Cage Trapping of the Mo-Centered Radical

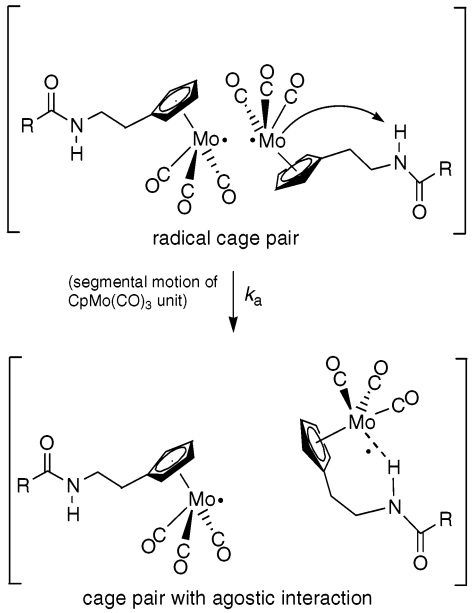

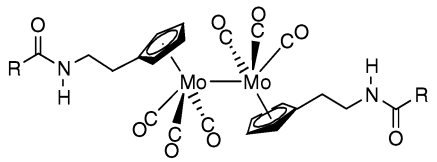

To our initial surprise, the F_{cP} values for the four radical cage pairs formed by photolysis of these complexes were essentially identical; i.e., there was no dependence of F_{cP} on the value of n. To explain this result, we hypothesized that, while still in the cage, the Mo radicals interacted with an H atom on the side chain to form a six-membered ring (Scheme 3). In effect, the metal radicals were captured in the cage. The cage recombination efficiencies were thus independent of *n* because the segmental motion of the Mo radical to form the agostic interaction[25] is independent of the chain length.[26]

(18) (a) Guillet, J. *Polymer Photophysics and Photochemistry*; Cambridge University Press: Cambridge, U.K., 1985; p 274. (b) The overall quantum yields decreased until a minimum value was reached, at which point a further increase in chain length did not lead to a decrease in quantum yield. At this point, segmental motion presumably dominates molecular motion rather than center-of-mass diffusion, so an increase in chain length will have little effect on the efficiency of the reaction.

(19) Guillet, J. *Adv. Photochem.* **1988**, *14*, 91−133.

(20) (a) The concept of the "cage effect" was introduced by Frank and Rabinowitch[20b−d] in 1934 to explain why the efficiency of I_2 photodissociation was smaller in solution than in the gas phase. It was proposed that the solvent temporarily encapsulates the reactive I• atoms in a "solvent cage", causing them to remain as colliding neighbors before they either recombine or diffuse apart. This concept is illustrated by the reaction in Scheme 2. The point to note is that the formation of free radicals is preceded by the formation of a caged radical pair. (b) Frank, J.; Rabinowitch, E. *Trans. Faraday Soc.* **1934**, *30*, 120−131. (c) Rabinowitch, E.; Wood, W. C. *Trans Faraday Soc.* **1936**, *32*, 1381−1387. (d) Rabinowitch, E. *Trans Faraday Soc.* **1937**, *33*, 1225−1233.

(21) (a) Koenig, T.; Fischer, H. *Free Radicals*; Kochi, J., Ed.; John Wiley: New York, 1973; Vol. 1, Chapter 4. (b) Koenig, T. *Organic Free Radicals*; Pryor, W. A., Ed.; ACS Symposium Series 69; American Chemical Society: Washington, DC, 1978; Chapter 9.

(22) (a) Male, J. L.; Lindfors, B. E.; Covert, K. J.; Tyler, D. R. *Macromolecules* **1997**, *30*, 6404−6406. (b) Male, J. L.; Lindfors, B. E.; Covert, K. J.; Tyler, D. R. *J. Am. Chem. Soc.* **1998**, *120*, 13176−13186.

(23) (a) Noyes, R. M. *J. Chem. Phys.* **1954**, *22*, 1349−1359. (b) Noyes, R. M. *Prog. React. Kinet.* **1961**, *1*, 129−160. (c) Noyes, R. M. *J. Am. Chem. Soc.* **1955**, *77*, 2042−2045. (d) Noyes, R. M. *J. Am. Chem. Soc.* **1956**, *78*, 5486−5490.

(24) Male, J. L.; Yoon, M.; Glenn, A. G.; Weakley, T. J. R.; Tyler, D. R. *Macromolecules* **1999**, *32*, 3898−3906.

(25) (a) Brookhart, M.; Green, M. L. H. *J. Organomet. Chem.* **1983**, *250*, 395. (b) Brookhart, M.; Green, M L. H.; Wong, L L. *Prog. Inorg. Chem.* **1988**, *36*, 1−124. (c) Yao, W.; Eisenstein, O.; Crabtree, R. H. *Inorg. Chim. Acta* **1997**, *254*, 105−111. (d) Crabtree, R. H.; Eisenstein, O.; Sini, G.; Peris, E. *J. Organomet. Chem.* **1998**, *567*, 7−11.

To test the in-cage trapping hypothesis and to further explore the dependence of F_{cP} on mass and chain length, we synthesized molecules **6**−**6** to **8**−**8** in which methyl groups replace the H atoms of **1**−**1** to **4**−**4**. No Mo···H agostic interactions are possible with these new complexes. This paper reports the results of our study.

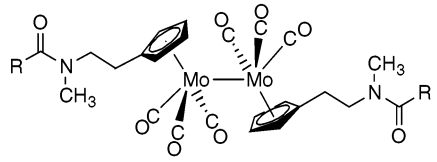

R = $(CH_2)_nCH_3$ with n = 3 (**6-6**), 8 (**7-7**), and 18 (**8-8**).

Results and Discussion

Syntheses of 6−6 to 8−8. Complexes **6**−**6** to **8**−**8** and their precursors were synthesized by modifying the synthetic route previously published for complexes **1**−**1** to **4**−**4** (Schemes 4−7).[24,27−29] Scheme 4 shows the synthesis of the methyl-substituted amine ligand that was used in Scheme 5. The amine was produced on the 100 g scale, in high purity, and with yields >80%. Reaction of the amine with sodium cyclopentadienide (Scheme 5) resulted in the substituted cyclopentadienyl ligand (40%), which was then reacted with $Mo(CO)_6$ (Scheme 6) to yield the indicated molybdenum dimer in yields over 50%. Molecules **6**−**6** to **8**−**8** were then completed by the route in Scheme 7. The complexes were purified by dissolving each in THF and then gravity filtering them through slow filter paper in the dark in a glovebox.

The $-CH_2CH_2-$ group present between the amide group and the Cp rings in these molecules is noteworthy. As previously discussed,[30] this spacer isolates the Mo−Mo chromophore from any electronic changes caused by varying the side chains on the Cp rings. By doing this, the resulting electronic spectra of the four complexes were virtually identical (see Experimental Section), suggesting that the changes in the photophysical parameters will be caused only by differences in the lengths of the side chains and not by electronic differences in the Mo−Mo bond chromophores.

Measurement of F_{cP}. F_{cP} was obtained using the method previously described.[31] In brief, the values for F_{cP} were extracted from quantum yield measurements of reaction 1 as a function

Scheme 4. Synthesis of $[BrCH_2CH_2NH_2CH_3][Br]$

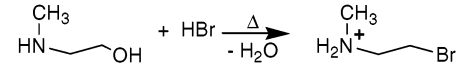

Scheme 5. Synthesis of $C_5H_5CH_2CH_2N(H)CH_3$

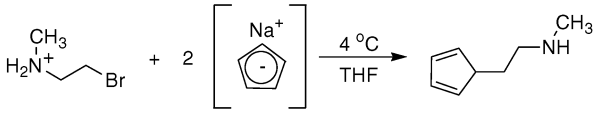

Scheme 6. Synthesis of $[(\eta^5\text{-}C_5H_4CH_2CH_2N(H)_2CH_3)_2Mo_2(CO)_6][NO_3]_2$

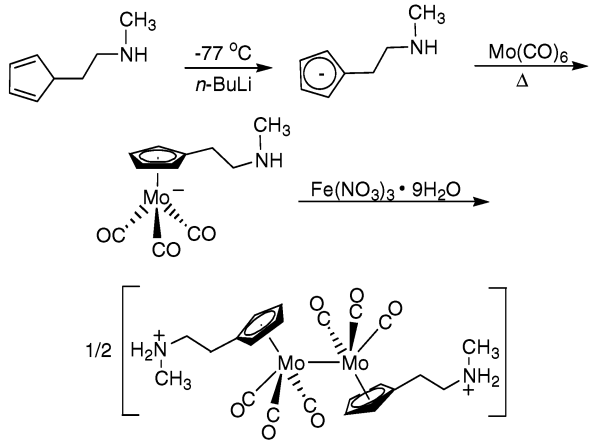

Scheme 7. Synthesis of Molecules **6**−**6** to **8**−**8** from $[(\eta^5\text{-}C_5H_4CH_2CH_2N(H)_2CH_3)_2Mo_2(CO)_6][NO_3]_2$

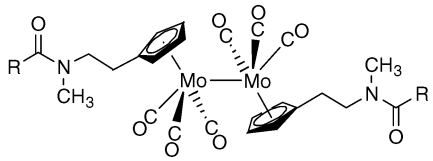

R = $(CH_2)_nCH_3$ with n = 3 (**6-6**), 8 (**7-7**), and 18 (**8-8**).

of solvent viscosity. (Solvent viscosity was modified by adding varying amounts of squalane to the hexanes/CCl_4 solvent.[32])

$$(RCp)_2Mo_2(CO)_6 \xrightarrow[\text{hexanes/squalane}]{h\nu\ (546\ \text{nm});\ CCl_4} 2(RCp)Mo(CO)_3Cl + [2CCl_3] \quad (1)$$

The quantum yields as a function of viscosity were then fit to eq 2, where c is a fitting parameter that contains k_{cP}, ϕ_{pair} is the quantum yield for formation of the radical cage pair, and ϕ_x is an offset parameter that is necessary to account for an

(26) While reversibility in the formation of the agostic species is suggested once the radicals are out of the solvent cage, the process need only be irreversible on the time scale of the cage processes, i.e., recombination and diffusion apart, to significantly diminish differences in F_{cP} among the four dimers.

(27) (a) Cortese, F. *Organic Syntheses*; Wiley: New York, 1943; Collect. Vol. 2, p 91. (b) Martin, S. F.; Puckette, T. A.; Colapret, J. A. *J. Org. Chem.* **1979**, *44*, 3391−3396. (c) Fries, K. M.; Joswig, C.; Borch, R. F. *J. Med. Chem.* **1995**, *38*, 2672−2680.

(28) (a) Hughes, A. K.; Meetsma, A.; Teuben, J. H. *Organometallics* **1993**, *12*, 1936−1945. Nieckarz, G. F.; Litty, J. J.; Tyler, D. R. *J. Organomet. Chem.* **1998**, *554*, 19−28.

(29) (a) Nieckarz, G. F.; Tyler, D. R. *Inorg. Chim. Acta* **1996**, *242*, 303−310.

(30) The $-CH_2-CH_2-$ spacer can viewed as an electronic insulator that reduces any electronic variations caused by differences in *n*, the number of $-CH_2-$ groups. For a similar use of this strategy see: Hughes, R. P.; Trujillo, H. A. *Organometallics* **1996**, *15*, 286−294. Note that each molecule has an intense band at ≈390 nm in THF ($\epsilon \approx 20\,000\ cm^{-1}\ M^{-1}$), assigned to the $\sigma \rightarrow \sigma^*$ transition, and a weaker band at ≈505 nm in THF ($\epsilon \approx 2000\ cm^{-1}\ M^{-1}$), assigned to a $d\pi \rightarrow \sigma^*$ transition. See ref 17a for a more in depth discussion of the electronic structures of these metal−metal-bonded molecules.

(31) (a) Braden, D. A.; Parrack, E. E.; Tyler, D. R. *Photochem. Photobiol. Sci.* **2002**, *1*, 418−420. (b) Braden, D. A.; Parrack, E. E., Tyler, D. R. *Coord. Chem. Rev.* **2001**, *21*, 279−294.

(32) In prior work, it was shown that in a sufficiently high concentration of CCl_4 (>0.1 M) all radicals that escape the solvent cage ("free radicals") were captured. Thus, formation of a thermal (collisional) cage pair and recombination of escaped (free) radicals becomes negligible. Under such conditions, the observed quantum yield (Φ_{obsd}) for the disappearance of the dimer is given by the following equation: $\Phi_{obsd} = \phi_{pair}[k_{dP}/(k_{cP} + k_{dP})] = \phi_{pair}[1 - F_{cP}]$, where ϕ_{pair} is the quantum yield for the formation of the cage pair ($\phi_{pair} = k_P/(k_P + \Sigma k_R)$) and $1 - F_{cP}$ is the fraction of radical pairs that escape the cage and subsequently are trapped by CCl_4. Rearrangement of this equation yields the following: $1/\Phi_{obsd} = [1/\phi_{pair}][1 + k_{cP}/k_{dP}]$. This equation shows that k_{cP}/k_{dP} (and in turn F_{cP}) can be calculated if ϕ_{pair} and Φ_{obsd} are known. Because Φ_{obsd} can be measured, the problem of determining F_{cP} is reduced to determining ϕ_{pair}, which can be found by measuring the quantum yields for the disappearance of the dimer as a function of viscosity. When the usual assumption is made that ϕ_{pair} and k_{cP} are independent of viscosity for a particular solvent system, and therefore that the only viscosity dependence arises from the diffusion of radicals out of the solvent cage, (k_{dP}), then according to the Stokes−Einstein−Smoluchowski equation $k_{dP} \propto D \propto 1/\eta$ and the previous equation thus becomes the following: $\Phi_{obsd} = [\phi_{pair}/(1 + \eta/c)] + \phi_x$.

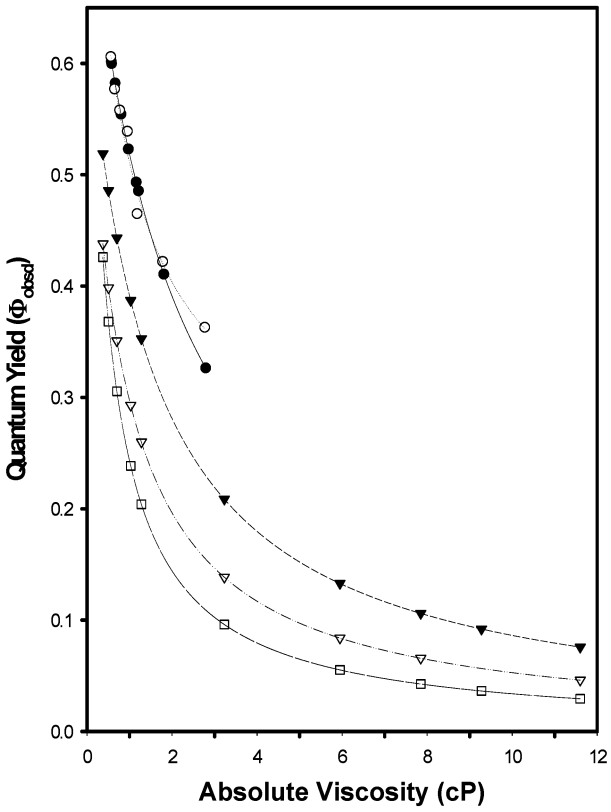

Figure 1. Plots of Φ_{obsd} vs viscosity for the photochemical reaction (λ = 546 nm) of molecules **1**−**1** to **4**−**4** (●), **5**−**5** (○), **6**−**6** (▼), **7**−**7** (▽), and **8**−**8** (□) with CCl_4 (≈2 M) at 23 ± 1 °C in hexanes/squalane. The previous Φ_{obsd} vs viscosity data for complexes **1**−**1** to **4**−**4** were so similar that to reduce clutter they have been reduced to a single set of data points, made up of the statistical averages of the Φ_{obsd} values for those molecules at the viscosity in question.

additional reaction that occurs in these systems.[33,34]

$$\Phi_{obsd} = [\phi_{pair}/(1 + \eta/c)] + \phi_x \qquad (2)$$

Chain Length Effects. Quantum yields for the photochemical reactions (λ = 546 nm) of **6**−**6** to **8**−**8** with CCl_4 as a function of solvent system viscosity are shown in Figure 1. Note that, at any selected viscosity, the quantum yields decrease as the chain length of the side chain on the Cp ligands increase in length. These results are in contrast to the quantum yields for the analogous photochemical reactions of complexes **1**−**1** to **4**−**4**. With these latter molecules, the quantum yields at any selected viscosity were independent of chain length, a result attributed to the in-cage trapping reaction described in the Introduction.

F_{cP} and ϕ_{pair} values for molecules **6**−**6** to **8**−**8** were extracted from the quantum yield data in Figure 1 using the procedure described in the preceding section. The resulting values are shown in Figure 2 and in Table S1 (Supporting Information). Note that, for any selected viscosity, F_{cP} follows the order **6**−**6** < **7**−**7** < **8**−**8**; i.e., F_{cP} increases as the side-chain length

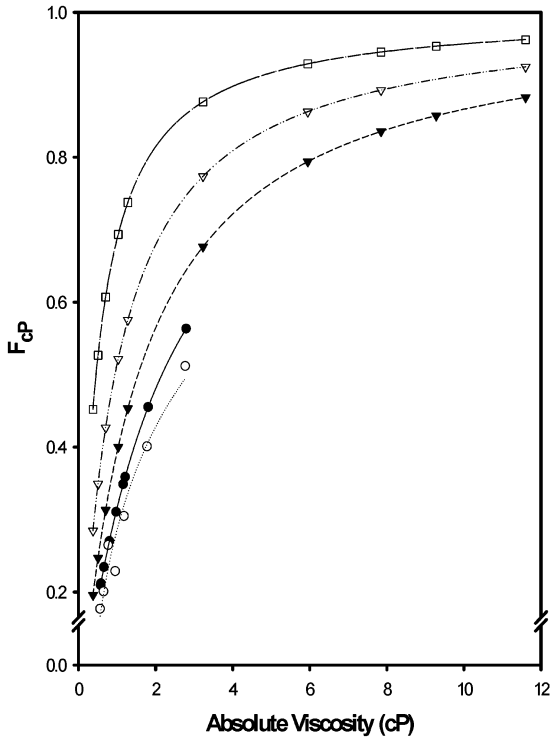

Figure 2. Plots of F_{cP} vs viscosity for cage pairs [**1**• •**1**] to [**4**• •**4**] (●), [**5**• •**5**] (○), [**6**• •**6**] (▼), [**7**• •**7**] (▽), and [**9**• •**9**] (□) at 23 ± 1 °C in hexanes/squalane. The previous F_{cP} vs viscosity data for complexes **1**−**1** to **4**−**4** were so similar that to reduce clutter they have been reduced to a single set of data points, made up of the statistical averages of the F_{cP} values for those molecules at the viscosity in question.

increases. An obvious point is that molecules **6**−**6** to **8**−**8** behave differently from molecules **1**−**1** to **4**−**4**, their H-containing analogues, in that the quantum yields and F_{cP} values for molecules **6**−**6** to **8**−**8** are not all the same. Because the quantum yields and F_{cP} values for **6**−**6** to **8**−**8** are different, it is concluded that no substantial "in-cage" trapping occurs with cage pairs [**6**•, •**6**], [**7**•, •**7**], and [**8**•, •**8**], as was expected from the replacement of H on the amide group by methyl. These results also support the "agostic interaction hypothesis" that was invoked to explain the fact that molecules **1**−**1** to **4**−**4** all have the same F_{cP} values at any selected viscosity.

Quantitative Interpretations. The relationship between F_{cP} and chain length can be quantified, at least approximately. As discussed in the Introduction, the ratio k_{dP}/k_{cP} (which is equal to $F_{cP}^{-1} - 1$) is linearly proportional to $m^{1/2}/r^2$ for cage pairs formed by photolysis of the $(CpCH_2CH_2OSiR_3)_2Mo_2(CO)_6$ molecules (R = Me, *i*-Pr, *n*-Pr, *n*-Hx). Figure 3 shows that a similar relationship holds for the [**6**•, •**6**], [**7**•, •**7**], and [**8**•, •**8**] cage pairs. Although this is just the second experimental verification of Noyes's prediction, the Noyes relationship is emerging as a rather general expression for predicting (or at least comparing) F_{cP} values.[35] It is important to not overinterpret the plots in Figure 3. Although Noyes predicted a linear relationship, the plot in Figure 3 may or may not be linear; the lack of more data points makes it difficult to say for certain. However, regardless of whether the relationship to $m^{1/2}/r^2$ is exactly linear, the important point is that k_{dP}/k_{cP} correlates in at

(33) As discussed in a prior paper,[31a] the ϕ_x parameter indicates that an additional reaction occurs, likely by an electron-transfer mechanism, in systems containing CCl_4. This additional mechanism results in a net reaction of the dimer starting material, even at very high viscosities where diffusion of the reactants is severely restricted.

(34) Note that in-cage trapping of the radical pair by CCl_4 is not likely. A comparison of rate constants for the reaction of $CpMo(CO)_3$ with CCl_4 (10^4 M^{-1} s^{-1}) with that for cage recombination (k_c) (≥10^9 s^{-1}) and with that for diffusional separation (k_d) (≈10^9−10^{10} s^{-1}) shows that the free radical trapping reaction cannot compete with the other two processes.

(35) A qualitative interpretation of the mass dependence is that heavier particles can shove aside solvent molecules more easily than lighter particles; hence, diffusion is favored for heavier particles. The dependence on r^2 is discussed in the text.

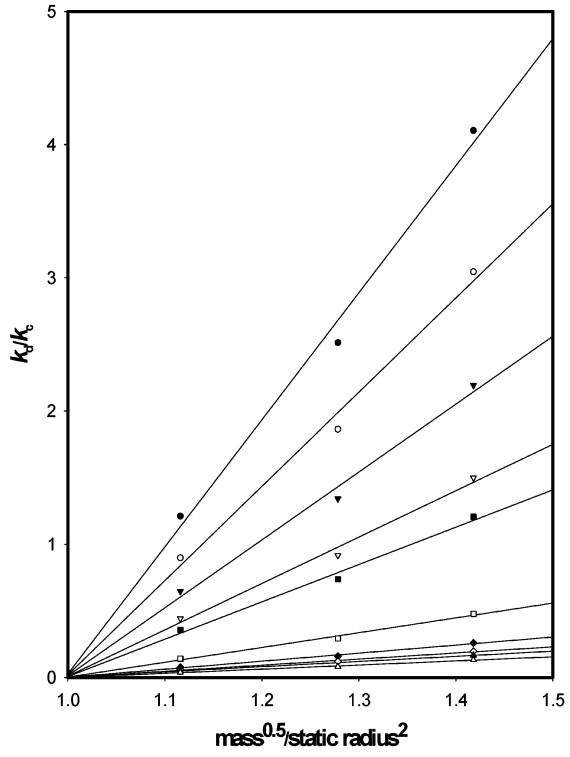

Figure 3. Plot of k_{cP}/k_{dP} vs $m^{1/2}/r^2$ (m = mass of the radical; r = the radius of a sphere with the same volume as the static volume of the radical) for radical cage pairs formed from molecules **6**−**6** to **8**−**8** at the measured viscosities of 0.376, 0.507, 0.704, 1.03, 1.28, 3.23, 5.95, 7.85, 9.28, and 11.6 cP (top to bottom).

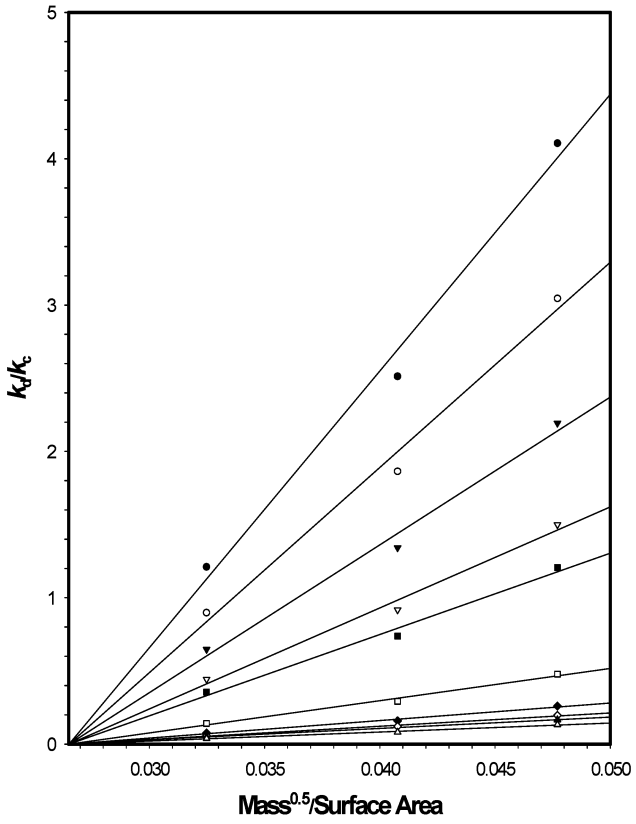

Figure 4. Plot of k_{cP}/k_{dP} vs $m^{1/2}$/(surface area) for radical cage pairs formed from molecules **6**−**6** to **8**−**8** at the measured viscosities of 0.376, 0.507, 0.704, 1.03, 1.28, 3.23, 5.95, 7.85, 9.28, and 11.6 cP (top to bottom).

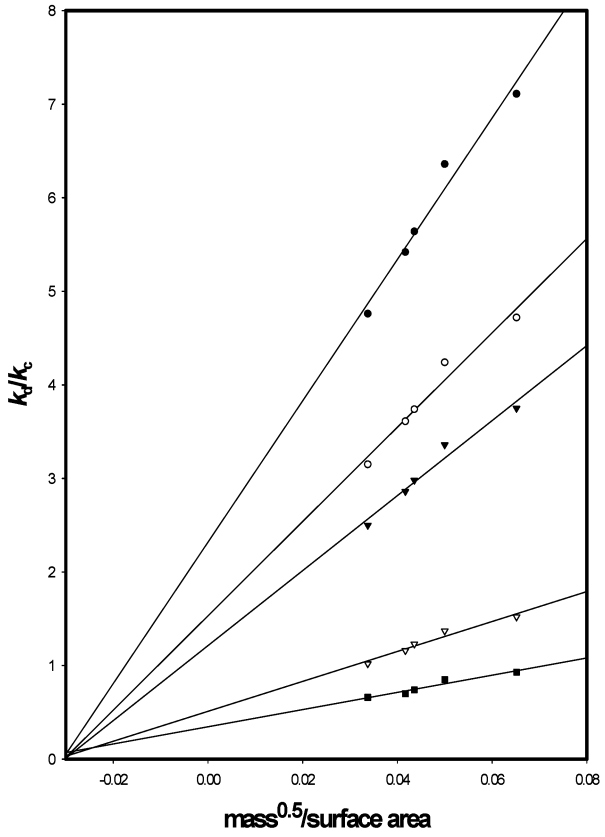

Figure 5. Plot of k_{cP}/k_{dP} vs $m^{1/2}$/(surface area) for radical cage pairs formed from molecules **1**−**1** to **5**−**5** at the measured viscosities of 0.47, 0.72, 0.90, 2.2, and 3.6 cP (top to bottom). Data are from ref 22b.

least an approximate way with the particles' mass$^{1/2}$ and radius^2. By knowing the (at least approximate) relationship between k_{dP}/k_{cP} and the mass and radius, one can reasonably predict the relative magnitudes of the cage effects for a series of radical cage pairs.

The interesting feature about the reasonably good linear fit between k_{dP}/k_{cP} and $m^{1/2}/r^2$ in Figure 3 is that Noyes derived his expression for spherical particles yet the radicals used in this study are decidedly not spherical. The explanation for the good fit lies in the reason for the dependence of F_{cP} on r^2. The parameter r^2 is proportional to the surface area of a particle, which in turn is proportional to the number of interactions a particle has with solvent molecules. The more interactions a particle has with the solvent, the greater the viscous drag and consequently the slower the rate of diffusion (and hence the inverse dependence of k_{dP}/k_{cP} on r^2). This analysis suggests that Noyes's expression can be modified by replacing r^2 with the particle's surface area, i.e., $k_{dP}/k_{cP} \propto m^{1/2}$/radical surface area. To test this suggestion, a plot of k_{dP}/k_{cP} vs $m^{1/2}$/surface area is shown in Figure 4. Note the reasonable linearity of the plots at the various viscosities, a result which suggests that using surface area instead of r^2 is acceptable. As a further test, k_{dP}/k_{cP} was plotted vs $m^{1/2}$/surface area for the $(CpCH_2CH_2OSiR_3)_2Mo_2(CO)_6$ molecules (R = Me, *i*-Pr, *n*-Pr, *n*-Hx; data from ref 22b). The results are shown in Figure 5; again, note that the plots are reasonably linear, which provides further support for the modified Noyes expression. The significance of being able to use a particle's surface area in the Noyes expression is that the expression becomes useful for nonspherical particles; i.e., it becomes possible to use the Noyes expression for virtually all

radicals and not just spherical ones. Further tests of the modified Noyes expression are proceeding in our laboratory.

Key Conclusions and Insights. The results in this study provide a second example showing that F_{cP} increases as the length of the chain on a radical center increases. This result provides at least one of the reasons why the quantum yields for photolytic polymer degradation (and long-chain molecules, in general) decrease as the polymer chains get longer. Quantitatively, the results herein show that the ratio k_{dP}/k_{cP} is approximately linearly proportional to mass$^{1/2}$/surface area. This relationship allows the approximate prediction of F_{cP} values for radicals of different sizes and masses. Undoubtedly, after a certain chain length and/or mass is reached, no changes in F_{cP} will be observed due to the vast inertia of the radicals, which forces their movements to be local and to not involve movement of the entire center of mass of the chain. We are currently working on the synthesis of the $n = 13$, 23, and 28 complexes, with the goal of determining at what chain length the F_{cP} values become independent of chain length.

Experimental Section

All manipulations were carried out in the absence of water and atmospheric oxygen using standard Schlenk line and glovebox techniques.

Materials and Reagents. Molybdenum hexacarbonyl, 2-(methylamino)ethanol, hydrobromic acid, *n*-butyllithium in cyclohexane, acetone (99.5%, spectrophotometric grade), sodium cyclopentadienide in THF (2.0 M), sodium sulfate, iron(III) nitrate nonahydrate, decanoic acid, and eicosanoic acid were obtained from Aldrich and used with further purification. Pentane (98%, Mallinckrodt) and methyl alcohol (anhydrous, Mallinckrodt) were used without further purification. THF (Burdick and Jackson) and hexanes (Fisher) were distilled from potassium benzophenone ketyl under nitrogen. Ethyl ether (Mallinckrodt) was distilled from sodium benzophenone ketyl under nitrogen. Ethyl chloroformate (Eastman), triethylamine (Merck), valeric acid (Aldrich), and squalane (Aldrich) were degassed with a nitrogen purge for 2 h prior to use. $CDCl_3$ and DMSO-d_6 (Cambridge Isotope) were distilled from CaH_2 under reduced pressure. $CDCl_3$ and CD_3OD (Cambridge Isotope) were used without further purification. CCl_4 (Fisher) was distilled twice from P_2O_5 and passed through a column of dry basic alumina prior to use. All solvents for quantum yield measurements were further degassed by three freeze−pump−thaw cycles and kept sealed in storage flasks in a darkened glovebox prior to use. Filter papers were either Fisherbrand P8 Qualitative or Whatman 5 Qualitative.

Instrumentation and Procedures. Infrared spectra were recorded on a Nicolet Magna 550 FT-IR spectrometer with OMNIC software. Samples were prepared as either KBr pellets or as solutions in CaF_2 cells (path length 0.110 mm). Electronic absorption spectra were recorded with a Hewlett-Packard 8453 UV−vis spectrophotometer. Mass spectral data were collected using both the electrospray and APCI heads in an Agilent 1100 series LC/MSD. Elemental analyses were performed by Atlantic Microlab, Inc., Norcross GA. The static molecular volumes for molecules **6**−**6** to **8**−**8** were estimated on the basis of the results obtained previously[22b] for **1**−**1** to **4**−**4** using the Steric[36] computer program. Maximum spherical volume calculations and maximum surface area estimates were made possible by creating minimized model complexes in the Spartan program. From these models, measurements of the longest molecular axis for the radical (i.e. the diameter of the sphere) were made and the surface area calculated using that specific option available in the program. The quantum yields ($\lambda = 546$ nm) for the formation of the cage pair and for the recombination efficiency were determined with an Oriel Merlin system equipped with an Oriel 200 W high-pressure mercury arc lamp as previously described.[22b,31a] The experimental method for obtaining F_{cP} from the quantum yields as a function of viscosity has been previously described[31a] but is repeated in the Supporting Information for convenience.

Photochemical Reactions of Complexes 6−6, 7−7, and 8−8. The three sets of 30, 3 mL, mixed-viscosity solutions used to obtain quantum yields for the reactions of **6**−**6** to **8**−**8** were prepared in airtight UV−visible cells in a darkened glovebox. The desired 2.4 mL ratio of both hexanes and squalane was first injected into each cell followed by preparation of a CCl_4 stock solution containing the dimer of study, of which each cell received 0.6 mL. (A new stock solution was made up for each new set of samples and was concentrated enough that when each 0.6 mL sample was diluted to 3.0 mL the resultant solution still gave an absorbance between 1.0 and 1.5 at 504 nm.) Each sample was then irradiated ($\lambda = 546$ nm) over a period of 20 min during which time 401 intensity observations were collected, of which the middle 200 observations between 5 and 15 min were used for the determination of quantum yields.

Synthesis of $BrCH_2CH_2N(H)CH_3 \cdot HBr$. The following is a more detailed preparation of a rather vague procedure that has been reported in the literature multiple times.[27] A 250 mL round-bottom flask was charged with a stirbar and 100 mL (0.883 mol) of HBr (48% w/w). The solution was cooled to 4 °C in a ice bath, and 35 mL (0.438 mol) of ice cold 2-(methylamino)ethanol was added dropwise with stirring. Because of the extreme exothermic nature of this reaction, special care was taken not to add the amine solution too quickly, reducing the chances of an explosive boil-over. The resulting mixture was then attached to a distillation apparatus that had a 2 in, fractionating column built into the distillation head, and the solution was brought to reflux by heating in an oil bath. As the bath temperature neared 150 °C, the head temperature reached 100 °C and distillation of H_2O began. The distillation was allowed to continue slowly (9−11 h) until ≈60 mL of distillate was collected. During this time, distillation was performed for ≈1 h, and then the oil bath was turned down to the point that reflux continued but distillation ceased for ≈30 min. (The distillation was stopped (but reflux continued) whenever the head temperature rose above 105 °C or dropped significantly below 100 °C, indicating an absence of water.) In our hands, the distillation/reflux process was repeated four times. When the solution no longer produced any distillate at a head temperature of 100 °C, the bath temperature was increased, the head temperature rose to ≈123 °C, and distillation of crude HBr began. Failure to distill off the remaining crude HBr at the conclusion of the synthesis inhibited the precipitation of the final product upon addition of cold acetone. The HBr distillation was continued for approximately 2 h, after which time the solution was allowed to cool. It is important to note that the appearance of a brown distillate is indicative of decomposition and the distillation should be stopped immediately and the solution cooled. After the solution had cooled to 60 °C, it was slowly poured with stirring into a 500 mL beaker containing 300 mL of ice cold acetone, whereupon the desired white product precipitated from solution. This heterogeneous solution was capped and placed in the freezer (−20 °C) overnight. The white precipitate was then vacuum filtered through a 60 mL medium-porosity sintered glass funnel, washed three times with 100 mL aliquots of ice cold acetone, and dried in the funnel, yielding 75.2 g (78%) of crude product. Reconcentration of the mother liquor followed by addition of another 200 mL of ice cold acetone yielded another 7.2 g of product bringing the crude yield to 82.4 g (86%). Further purification was achieved by using a mortar and pestle to crush the crude product, followed by rinses with 50 mL aliquots of ice cold acetone until the filtrate ran clear, yielding 80.3 g (83%). ^{1}H NMR ($CDCl_3$): δ 9.23 (t, 2H, $BrCH_2CH_2N(H)_2CH_3$), 3.83 (t, 2H, $BrCH_2CH_2N(H)_2CH_3$), 3.47 (t, 2H, $BrCH_2CH_2N(H)_2CH_3$), 2.82 (s, 3H, $BrCH_2CH_2N(H)_2CH_3$). An

(36) The computer program Steric was written by B. Craig Taverner, Department of Chemistry, Witwatersrand, Private Bag 3, WITS 2050, Johannesburg, South Africa.

X-ray crystal structure also confirmed the structural identity of this molecule (Figure S1; see Supporting Information).

Synthesis of $C_5H_5CH_2CH_2N(H)CH_3$. A 500 mL, dry Schlenk flask was charged with a stirbar and 17.5 g (0.080 mol) of $BrCH_2CH_2N(H)CH_3 \cdot HBr$. The flask was sealed with a rubber septum, and 250 mL of freshly distilled, deoxygenated THF was added by cannula. The white heterogeneous solution was cooled to 4 °C in an ice bath, and sodium cyclopentadienide (80.0 mL, 0.160 mol) was added dropwise through a syringe. The milky, purple solution was covered to minimize exposure to light and allowed to slowly come to room temperature. After the solution was stirred for 48 h, it was noted that the solution had retained its milky purple appearance. (A change to brown or orange at this point in the reaction indicated significant decomposition, most likely from the presence of oxygen.) Deoxygenated distilled water (≈100 mL) was then cannulated into the solution until it became homogeneous. The resultant mixture was then cannulated into a 1 L separatory funnel, which had been capped with a rubber septum and purged with N_2 prior to use. The aqueous layer was removed and freshly distilled ethyl ether (200 mL) was added by cannula. Deoxygenated distilled water (100 mL) was then cannulated into the solution, and the combined mixture was shaken vigorously with venting for 1 min. The water layer was then removed and the process repeated with another 100 mL aliquot of water. After the water layer was removed a second time, the separatory funnel held the organic layer and a insoluble layer of dark brown solids. These solids were also drained off, leaving behind the clear, green/orange organic layer. This solution was cannulated into a 500 mL round-bottom flask, which had been charged with sodium sulfate (≈30 g). The heterogeneous mixture was shaken lightly to promote the drying process and left to sit in the dark for 1 h, after which time the organic mixture was gravity filtered in the air through fast filter paper into a 1 L round-bottom flask. The solvent was removed by rotary evaporation, leaving a viscous orange/brown oil. The oil was transferred via pipet into a 100 mL round-bottom flask that had been charged with a stirbar, and the desired product, a clear, colorless oil, was obtained by distillation at 35−40 °C under reduced pressure, yielding 3.94 g (0.032 mol, 40%). Because of the instability of the product, (a yellow tint is indicative of decomposition), it is suggested that it be used immediately or stored under N_2 in the dark at −20°C. ^{1}H NMR ($CDCl_3$) showed the purified product to be a 1:1 mixture of two ring isomers with the alkyl group attached to the cyclopentadiene ring in the 1 and 2 positions:[37] δ 6.41 (m, 3H, 2 × CH of C_5H_5 ring isomer 1, 1 × CH of C_5H_5), 6.26 (m, 1H, CH of C_5H_5 ring isomer 2), 6.23 (t, 1H, CH of C_5H_5 ring isomer 2), 6.06 (t, 1H, CH of C_5H_5 ring isomer 1), 2.95 (d, 2H, CH_2 of C_5H_5 ring isomer 1), 2.88 (d, 2H, CH_2 of C_5H_5 ring isomer 2), 2.75 (q, 2H, $C_5H_5CH_2CH_2N(H)CH_3$), 2.57 (m, 2H, $C_5H_5CH_2CH_2N(H)CH_3$), 2.41 (s, 3H, $C_5H_5CH_2CH_2N(H)CH_3$), 1.83 (b s, 2H, 2 × $C_5H_5CH_2CH_2N(H)CH_3$).

Synthesis of $[(\eta^5\text{-}C_5H_4CH_2CH_2N(H)_2CH_3)_2Mo_2(CO)_6][NO_3]_2$. The $[\eta^5\text{-}C_5H_4CH_2CH_2N(H)_2CH_3]_2Mo_2(CO)_6[NO_3]_2$ precursor complex was synthesized with several key modifications to the previously reported procedure.[24] Freshly distilled THF (50 mL) was combined with $C_5H_5CH_2CH_2N(H)CH_3$ (7.5 g, 60.4 mmol) in a 100 mL Schlenk flask, which had been charged with a stirbar. The flask was capped with a tight-fitting rubber septum and degassed by two freeze−pump−thaw cycles. While the reaction mixture was still very cold (still in the liquid state), it was placed in a dry ice/acetone bath (−77 °C) and 6 mL of *n*-butyllithium solution (10 M in hexanes, 60.6 mmol) was added dropwise via syringe with stirring. The resulting solution was allowed to warm to room temperature and then stirred under N_2 for 1 h. In previous syntheses, the $Mo(CO)_6$ was added to the ligand/THF/*n*-butyllithium solution through a sidearm under a counter-flow of N_2. To better maintain an air-free environment, the $Mo(CO)_6$ (15.9 g, 60.4 mmol) was placed in a separate 500 mL three-neck flask charged with a stirbar. The middle neck of the flask was capped with a water cooled condenser, which was itself capped with an N_2 adapter. The two side-necks were capped by a tight-fitting rubber septum and another N_2 adapter, respectively. The apparatus was then evacuated and filled with N_2. Freshly distilled and degassed THF (150 mL) was then cannulated into the three-neck flask, and the resulting mixture was stirred. The amine/*n*-BuLi/THF solution, which contained a white suspension after stirring for 1 h, was slowly cannulated into the three-neck flask containing the $Mo(CO)_6$. During cannulation, the solution changed from clear to yellow to orange/yellow. The rubber septum was then replaced by a clear glass stopper under a strong N_2 counter-flow, and the resulting solution was brought to reflux under N_2, during which time the color changed from orange/yellow to dark red with a bright yellow precipitate evident along the edges of the solution. After 48 h, the solution was cooled to room temperature and concentrated to ≈100 mL in vacuo. From this point on, all steps were completed under a red light, with great care being taken to reduce any and all exposure to white light. The glass stopper was replaced by another tight-fitting rubber septum, and a solution of $Fe(NO)_3 \cdot 9H_2O$ (24.5 g in 150 mL of deoxygenated H_2O) was slowly cannulated into the solution with stirring. A dark red solid precipitated immediately upon addition of the iron nitrate solution, and the flask was placed in an ice bath overnight. The solid was filtered in the air through a 60 mL sintered glass funnel and washed with three 100 mL aliquots of ice cold, deoxygenated distilled water, followed by two 25 mL aliquots of ice cold deoxygenated methanol and one 100 mL aliquot of ice cold deoxygenated pentane. The product was placed in a 250 mL Schlenk flask and dried in vacuo for 24 h. Any excess $Mo(CO)_6$ was then removed by sublimation onto a liquid-nitrogen-cooled coldfinger, yielding 11.3 g (51%) of crude product. ^{1}H NMR (DMSO-d_6) showed the product to be a mixture of at least two rotamers:[38] δ 8.39 (s br, 4H, $C_5H_4CH_2CH_2N(H)_2CH_3$), 5.71 (br s, 4H, $C_5H_4CH_2CH_2N(H)_2CH_3$), 5.63 (br s, 8H, $C_5H_4CH_2CH_2N(H)_2CH_3$), 5.31 (br s, 4H, $C_5H_4CH_2CH_2N(H)_2CH_3$), 3.03 (m, 4H, $C_5H_4CH_2CH_2N(H)_2CH_3$), 2.71 (m, 4H, $C_5H_4CH_2CH_2N(H)_2CH_3$), 2.59 (s, 6H, $C_5H_4CH_2CH_2N(H)_2CH_3$). UV−vis (CH_3OH; λ_{max}, nm): 504, 389. MS (electrospray): *m*/*z* 606 (P − 2(NO_3)). IR (KBr, cm^{-1}): ν(CO) 2011 (w), 1954 (s), 1914 (s), 1881 (s); $\nu(NO_3^-)$ 1384 (s). Anal. Calcd for $Mo_2C_{22}H_{26}N_4O_{12}$: C, 36.18; H, 3.58. Found: C, 35.99; H, 3.57.

Synthesis of $[\eta^5\text{-}C_5H_4CH_2CH_2N(CH_3)CO(CH_2)_nCH_3]_2Mo_2(CO)_6$ (6−6, 7−7, 8−8). These complexes were synthesized from $[\eta^5\text{-}C_5H_4CH_2CH_2N(H)_2CH_3]_2Mo_2(CO)_6[NO_3]_2$ under red light using the procedure previously described for complexes **1**−**1** to **4**−**4**.[24] Purification was carried out in the glovebox by dissolving the crude product in 20−25 mL of freshly distilled freeze−pump−thawed THF and then gravity filtering the solution through slow filter paper. The resulting filtrate was concentrated in vacuo (≈5 mL), layered with hexanes (≈100 mL), capped with a glass stopper, and placed in the freezer overnight to facilitate precipitation of product. The complexes were vacuum filtered through 15 mL medium sintered glass funnels in the glovebox and dried under vacuum for 12 h. The precipitated complexes contained variable amounts of water molecules that could not be removed by further drying in vacuo. ^{1}H NMR spectra showed all three purified products to be mixtures of at least two rotamers.[38]

$[\eta^5\text{-}C_5H_4CH_2CH_2N(CH_3)CO(CH_2)_3CH_3]_2Mo_2(CO)_6$. Yield: 45%. IR (KBr; cm^{-1}): ν(CO) 2007 (w), 1947 (br, s), 1904 (sh), 1890 (s), 1870 (sh); ν(N(C═O)CH_3−): 1640 (m). ^{1}H NMR ($CDCl_3$): δ 5.25 (m, 8H, $C_5H_4CH_2CH_2N(CH_3)$−), 3.49 (m, 4H, $C_5H_4CH_2CH_2N(CH_3)$−), 2.95 (m, 6H, $C_5H_4CH_2CH_2N(CH_3)$−), 2.64 (m, 4H, $C_5H_4CH_2CH_2N(CH_3)$−), 2.32 (t, 4H, $C_5H_4CH_2CH_2N(CH_3)COCH_2CH_2CH_2CH_3$), 2.19 (t, 4H, $C_5H_4CH_2CH_2N(CH_3)COCH_2CH_2CH_2CH_3$), 1.61 (m, 4H, $C_5H_4CH_2CH_2N(CH_3)COCH_2CH_2CH_2CH_3$), 1.33 (m, 4H, $C_5H_4CH_2CH_2N(CH_3)COCH_2CH_2CH_2CH_3$), 0.96 (m, 4H, $C_5H_4CH_2CH_2N(CH_3)COCH_2$-

(37) (a) Kaul, B. B.; Noll, S.; Renshaw, S.; Rakowski Dubois, M. *Organometallics* **1997**, *16*, 1604−1611. (b) Hughes, A. K.; Meetsma, A.; Teuben, J. H. *Organometallics* **1993**, *12*, 1936.

(38) (a) Adams, R. D.; Collins, D. M.; Cotton, F. A. *Inorg. Chem.* **1974**, *13*, 1086−1090. (b) Adams, R. D.; Cotton, F. A. *Inorg Chim. Acta* **1973**, *7*, 153−156.

$CH_2CH_2CH_3$). Anal. Calcd for $Mo_2C_{32}H_{40}N_2O_8 \cdot 1/2H_2O$: C, 49.18; H, 5.29; N, 3.58. Found: C, 49.00; H, 5.15; N, 3.59. MS (APCI): *m*/*z* 773 (P^+).

[η^5-$C_5H_4CH_2CH_2N(CH_3)CO(CH_2)_8CH_3]_2Mo_2(CO)_6$. Yield: 38%. ^{1}H NMR ($CDCl_3$): δ 5.21 (m, 8H, $C_5H_4CH_2CH_2N(CH_3)-$), 3.46 (m, 4H, $C_5H_4CH_2CH_2N(CH_3)-$), 2.95 (m, 6H, $C_5H_4CH_2CH_2N(CH_3)-$), 2.62 (m, 4H, $C_5H_4CH_2CH_2N(CH_3)-$), 2.28 (t, 4H, $C_5H_4CH_2CH_2N(CH_3)COCH_2CH_2CH_2CH_3$), 2.16 (t, 4H, $C_5H_4CH_2CH_2N(CH_3)COCH_2CH_2CH_2CH_3$), 1.58 (m, 4H, $C_5H_4CH_2CH_2N(CH_3)COCH_2CH_2CH_2CH_3$), 1.27 (m, 4H, $C_5H_4CH_2CH_2N(CH_3)COCH_2CH_2CH_2CH_3$), 0.89 (m, 4H, $C_5H_4CH_2CH_2N(CH_3)COCH_2CH_2CH_2CH_3$). IR (KBr; cm^{-1}): ν(CO) 2007 (w), 1946 (s), 1916 (s), 1903 (sh), 1894 (s), 1870 (sh); ν(N(C═O)-CH_3-) 1634 (m). Anal. Calcd for $Mo_2C_{42}H_{60}N_2O_8 \cdot 1/2H_2O$: C, 54.72; H, 6.67; N, 3.04. Found: C, 54.66; H, 6.55; N, 3.16. MS (APCI): *m*/*z* 858 (P − 2(CO)).

[η^5-$C_5H_4CH_2CH_2N(CH_3)CO(CH_2)_{18}CH_3]_2Mo_2(CO)_6$. Yield: 47%. ^{1}H NMR ($CDCl_3$): δ 5.24 (m, 8H, $C_5H_4CH_2CH_2N(CH_3)-$), 3.49 (m, 4H, $C_5H_4CH_2CH_2N(CH_3)-$), 2.95 (m, 6H, $C_5H_4CH_2CH_2N(CH_3)-$), 2.64 (m, 4H, $C_5H_4CH_2CH_2N(CH_3)-$) 2.31 (t, 4H, $C_5H_4CH_2CH_2N(CH_3)COCH_2CH_2CH_2CH_3$), 2.17 (t, 4H, $C_5H_4CH_2CH_2N(CH_3)COCH_2CH_2CH_2CH_3$), 1.62 (m, 4H, $C_5H_4CH_2CH_2N(CH_3)COCH_2CH_2CH_2CH_3$), 1.29 (m, 4H, $C_5H_4CH_2CH_2N(CH_3)COCH_2CH_2CH_2CH_3$), 0.91 (m, 4H, $C_5H_4CH_2CH_2N(CH_3)COCH_2CH_2CH_2CH_3$). IR (KBr; cm^{-1}): ν(CO) 2008 (w), 1947 (s), 1914 (s), 1906 (sh), 1895 (s), 1888 (sh), 1870 (sh); ν(N(C═O)CH_3-) 1634 (m). Anal. Calcd for $Mo_2C_{62}H_{100}N_2O_8 \cdot 2.2H_2O$: C, 60.39; H, 8.53; N, 2.27. Found: C, 59.95; H, 7.88; N, 2.46. MS (APCI): *m*/*z* 1138 (P − 2(CO)).

Acknowledgment. The National Science Foundation is acknowledged for the support of this work.

Supporting Information Available: Tables of selected mass and photochemical data, mass and volume data for the radicals and solvents, crystallographic information for the $BrCH_2CH_2N(H)CH_3 \cdot HBr$ molecule, atomic coordinates and equivalent isotropic thermal parameters, bond lengths and angles, and anisotropic thermal parameters, an ORTEP drawing of the $BrCH_2CH_2N(H)CH_3 \cdot HBr$ molecule, and a description of the crystal structure analysis. This material is available free of charge via the Internet at http://pubs.acs.org.

JA035030R